

# Attachment of a Hydrophobically Modified Biopolymer at the Oil–Water Interface in the Treatment of Oil Spills

Pradeep Venkataraman,<sup>†</sup> Jingjian Tang,<sup>†</sup> Etham Frenkel,<sup>†</sup> Gary L. McPherson,<sup>‡</sup> Jibao He,<sup>§</sup> Srinivasa R. Raghavan,<sup>||</sup> Vladimir Kolesnichenko,<sup>⊥</sup> Arijit Bose,<sup>⊗</sup> and Vijay T. John<sup>\*,†</sup>

<sup>†</sup>Department of Chemical and Biomolecular Engineering, <sup>‡</sup>Department of Chemistry, and <sup>§</sup>Coordinated Instrumentation Facility, Tulane University, New Orleans, Louisiana 70118, United States

<sup>||</sup>Department of Chemical and Biomolecular Engineering, University of Maryland, College Park, Maryland 20742, United States

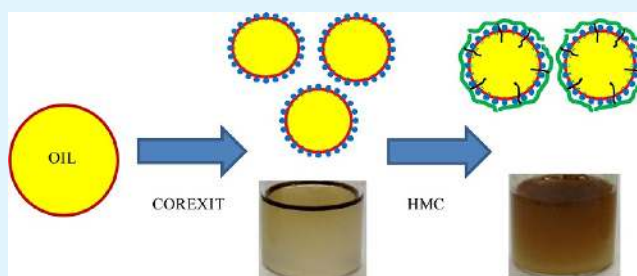
<sup>⊥</sup>Department of Chemistry, Xavier University of Louisiana, New Orleans, Louisiana 70125, United States

<sup>⊗</sup>Department of Chemical Engineering, University of Rhode Island, Kingston, Rhode Island 02881, United States

## S Supporting Information

**ABSTRACT:** The stability of crude oil droplets formed by adding chemical dispersants can be considerably enhanced by the use of the biopolymer, hydrophobically modified chitosan. Turbidimetric analyses show that emulsions of crude oil in saline water prepared using a combination of the biopolymer and the well-studied chemical dispersant (Corexit 9500A) remain stable for extended periods in comparison to emulsions stabilized by the dispersant alone. We hypothesize that the hydrophobic residues from the polymer preferentially anchor in the oil droplets, thereby forming a layer of the polymer around the droplets. The enhanced stability of the droplets is due to the polymer layer providing an increase in electrostatic and steric repulsions and thereby a large barrier to droplet coalescence. Our results show that the addition of hydrophobically modified chitosan following the application of chemical dispersant to an oil spill can potentially reduce the use of chemical dispersants. Increasing the molecular weight of the biopolymer changes the rheological properties of the oil-in-water emulsion to that of a weak gel. The ability of the biopolymer to tether the oil droplets in a gel-like matrix has potential applications in the immobilization of surface oil spills for enhanced removal.

**KEYWORDS:** oil spill, remediation, stability, dispersion, biopolymer, Corexit, modified chitosan, dispersant, crude oil, molecular weight, gel



## 1. INTRODUCTION

Dispersants are mixtures of surfactants that significantly reduce the interfacial tension between crude oil and water, thereby facilitating the creation of small oil droplets with low energy input provided naturally by wave actions and wind shear.<sup>1,2</sup> The entrainment of the surface slick into the water column is necessary for mitigating the impact of oil on the shores and aquatic fauna.<sup>2,3</sup> Another objective of using dispersants is to enhance the mixing of oil in the water column and its exposure to the benthic biota for degradation by natural means.<sup>2</sup> Corexit 9500A is one of the most commonly used dispersants in the United States for marine oil spill remediation. It is a mixture of nonionic surfactants (48%) and anionic surfactant (35%) in a solvent medium containing light hydrocarbon distillates and 1-(2-butoxy-1-methylethoxy) propanol.<sup>4</sup> The nonionic surfactants in Corexit 9500A are derivatives of polyethoxylated sorbitan and oleic acid. Dioctyl sodium sulfosuccinate commonly known as DOSS or AOT is the anionic surfactant that constitutes the Corexit class of dispersants.<sup>5–7</sup> Recent studies have indicated that Corexit 9500A is effective in dispersing different types of crude oil under varying conditions

of temperature and dissipation energy,<sup>8–11</sup> with a significant decrease in oil–water interfacial tension.<sup>6</sup> However, it has been shown that droplets formed using Corexit 9500A rapidly coalesce because of an insufficient electrostatic repulsive barrier.<sup>12</sup> It is therefore necessary to enhance the stability of the dispersed oil droplets, defined as the resistance to coalescence and determined by droplet hydrodynamics and colloidal interactions.<sup>1</sup>

Our objective in the current study is to apply an interesting concept where natural additives such as polysaccharides, are attached to oil droplets to enhance the stability of the droplets and potentially reduce the amount of dispersant required for effective dispersion of crude oil. The specific polymer we have used is hydrophobically modified chitosan (HMC). Chitosan is a linear chain polysaccharide consisting of n-glucosamine monomers connected through 1–4  $\beta$  linkages obtained by deacetylation of chitin, a naturally occurring polymer found in

Received: December 6, 2012

Accepted: March 25, 2013

Published: March 25, 2013

the shells of most crustaceans.<sup>13,14</sup> The polymer is soluble in slightly acidic aqueous media through protonation of the amine groups ( $pK_a \sim 6-6.5$ ) which also imparts cationic properties to the polymer.<sup>13</sup> Chitosan and derivatives of chitosan are biocompatible<sup>15</sup> and have been investigated for applications in drug delivery,<sup>16</sup> hemostasis,<sup>17</sup> and tissue engineering.<sup>18</sup> The emulsifying properties of chitosan and its derivative have been studied for applications in food industries<sup>19,20</sup> and as flocculating agents.<sup>21</sup> McClements and co-workers have shown that chitosan can form stable oil-in-water emulsions in the presence of anionic surfactants at low oil to water volume ratios.<sup>20</sup> A recent pioneering report indicates that chitosan can form a network with bacteria at the oil-water interface thereby forming oil-in-water Pickering emulsions stabilized by bacteria at the interface.<sup>22</sup> Although, chitosan has negligible interfacial activity, it enhances the stability of emulsions by a combination of mechanisms involving electrostatic repulsion and steric hindrance.<sup>23,24</sup>

The interfacial properties of the cationic chitosan can be altered by chemical modification.<sup>25,26</sup> In particular, hydrophobic residues such as alkyl chains can be attached to the polymer backbone by reductive amination.<sup>27</sup> Hydrophobic modification of chitosan makes the polymer amphiphilic and thereby interfacially active. In turn, the biopolymer has the ability to noncovalently link with hydrophobic materials using the alkyl chains as "hooks". For example, it has been shown that HMC chains, when added to a solution of vesicles, create a vesicular gel by bridging vesicles into a network where the vesicles are the nodes or cross-links.<sup>28</sup> A similar gelling effect has been found upon the addition of HMC to carbon microspheres, where the alkyl groups of HMC attach to the carbon particles through hydrophobic interactions.<sup>28,29</sup>

In this paper, we extend the above concepts to enhancing the stability of the crude oil droplets dispersed by the application of Corexit 9500A. We hypothesize that with lower molecular weight HMC at low concentrations, the polymer will anchor to droplets through its hydrophobes. As suggested by the schematic in Figure 1, the polymer chains may adsorb on the droplets and present a shell around individual droplets to

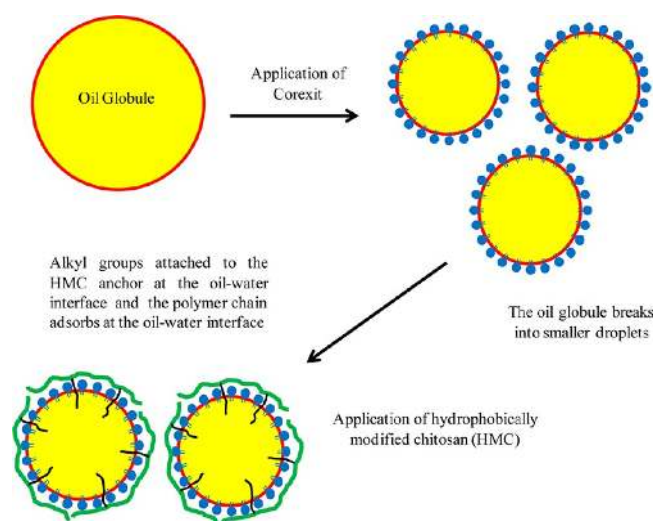


**Figure 1.** Schematic showing hydrophobically modified chitosan (HMC) molecules stabilizing dispersed oil droplets by anchoring the covalently attached alkyl groups at the oil-water interface and forming a protective layer around the oil droplet.

stabilize them against coalescence through steric and electrostatic repulsion. The application of dispersants, necessary for creation of small droplets by reduction of the interfacial tension, is followed by the application of the modified polysaccharide, which we show provides a barrier to rapid coalescence and resurfacing of the oil droplets. We also show that at higher molecular weights and concentrations, the polymer spans droplets resulting in a gel-like phase that may be of relevance to immobilizing surface oil for ease in removal.

## 2. EXPERIMENTAL SECTION

**2.1. Chemicals.** Low molecular weight chitosan (75–85% deacetylated, M.W. 50–190K Da), high molecular weight chitosan (>75% deacetylated, M.W. 310–375K Da), *n*-dodecyl aldehyde (92%) and sodium cyanoborohydride (reagent grade, 95%) were obtained from Sigma Aldrich and used as received without any further treatment. Deionized (DI) water, produced from an Elga water purification system (Medica DV25) with resistance of 18.2 M $\Omega$ , was used in the synthesis of hydrophobically modified chitosan. Louisiana sweet crude oil was obtained from British Petroleum's Macondo prospect (SOB-20100617032). Corexit 9500A (Nalco Energy Services) was used as received as the chemical dispersant in all experiments and is hereafter designated as Corexit. Saline water containing 0.6 M sodium chloride (Certified ACS grade, Fisher Scientific) was used as a substitute for seawater and was used in all experiments as the continuous phase.

**2.2. Synthesis of Hydrophobically Modified Chitosan (HMC).** Chitosan was hydrophobically modified by attaching the dodecyl chains to the amine groups on the polymer backbone following the procedures reported in the literature.<sup>27</sup> Briefly, *n*-dodecyl aldehyde was added to chitosan dissolved in acidic solution containing water and ethanol. The molar ratio of the aldehyde to glucosamine monomers was 0.025. The pH of the mixture was maintained as 5.0 to prevent the precipitation of chitosan. Following the addition of sodium cyanoborohydride, the solution was stirred for 24 h. Hydrophobically modified chitosan (HMC) was precipitated by adjusting the pH to 7 by adding sodium hydroxide solution. The precipitate was repeatedly washed with water and ethanol to remove excess reactants and then air-dried. The structure of hydrophobically modified chitosan and its <sup>1</sup>H nuclear magnetic resonance (NMR) spectrum are presented in Supporting Information, Figure S-1. The spectrum confirms the hydrophobic substitution on the polymer backbone and is in agreement with the literature.<sup>27,29</sup> Hydrophobically modified low molecular weight chitosan is designated as LHMC while the high molecular weight variant is designated as HHMC.

**2.3. Measurement of Interfacial Tension.** The addition of Corexit results in the reduction of interfacial tension between saline water and crude oil by several orders of magnitude.<sup>6</sup> Because of the wide range of interfacial tension and instrument limitations, two different techniques were employed in its measurement. Interfacial tension between crude oil and saline water was measured using the pendant drop method on a standard goniometer (ramé-hart Model 250), and the analysis was carried out using the DROPimage Advanced Software. For extremely low interfacial tensions of the dispersant-oil mixtures not accessible by the pendant drop method, the interfacial tension was measured using the spinning drop tensiometer (Grace Instruments model M6500). The spinning drop tensiometer uses a rotating capillary of 2 mm inner diameter with total volume of 0.292 cm<sup>3</sup>. In two separate sets of experiments, Corexit was mixed with saline water and crude oil respectively in various dispersant to oil volume ratios. Approximately 0.001 cm<sup>3</sup> of the less dense phase (crude oil or dispersant-oil mixture) was injected into the capillary filled with the more dense phase (saline water or dispersant-saline water mixture) using a micro syringe to create a small drop. The capillary tube was sealed and rotated at a velocity in the range of 5000–6000 rpm. The temperature of the tube was maintained at 25 °C by circulating cold water around the capillary tube. Droplet radii were measured using an optical microscope fitted with a digital output. Measurements of

interfacial tension with a spinning drop tensiometer are based on Vonnegut's formula:<sup>30</sup>

$$\gamma = \frac{\Delta\rho\omega^2R^3}{4} \quad (1)$$

where  $\gamma$  (mN m<sup>-1</sup>) is the interfacial tension,  $\Delta\rho$  (g cm<sup>-3</sup>) is the density difference between the drop and the surrounding fluid,  $\omega$  (rad s<sup>-1</sup>) is the angular velocity, and  $R$  (cm) is the drop radius. The formula has been shown to be valid within 0.1% accuracy if the drop is in equilibrium and the length of the drop exceeds four times its diameter. In a separate set of experiments, Corexit was mixed with crude oil in two different dispersant to oil volume ratios, and an acidic solution (pH = 4) containing 1 wt % LHMC was added to the saline water in varying mass ratios of HMC to Corexit. The interfacial tension between the oil phase and the saline water was measured using the spinning drop tensiometer as described above.

**2.4. Turbidimetric Measurements.** Measurement of the turbidity of an emulsion as a function of time is a useful tool in determining the stability of the dispersed phase. In our experiments, Corexit was mixed with crude oil in varying dispersant to oil volume ratios. The mixture of oil and dispersant was then added to a vial containing saline water. The oil to water volume ratio in all experiments was maintained as 0.003. The vial was stirred for 30 s on a vortex mixer (Thermolyne Maxi Mix II, 37W) at 3000 rpm. A small aliquot (~1.5 mL) of the emulsion was immediately transferred to a quartz cuvette (path length = 10 mm), and the transmittance of light ( $\lambda=400$  nm) through the emulsion was measured as function of time using a UV-vis Spectrophotometer (Shimadzu UV-1700).<sup>31</sup> Data was analyzed using UV Probe software (version 2.32). In a different set of experiments an acidic solution (pH = 4) containing 1 wt % LHMC was added to the vial following the addition of the mixture of Corexit and crude oil. The turbidity of the emulsion phase was measured as described above for varying mass ratios of LHMC to Corexit.

**2.5. Cryo-Scanning Electron Microscopy (SEM).** A mixture of crude oil and Corexit (dispersant to oil volume ratio 0.01) was added to a vial containing saline water. The oil to water volume ratio in the vial was 0.01. An acidic solution of LHMC was then added to the vial, the mass ratio of HMC to dispersant being 1. The vial was then stirred using a vortex mixer for 1 min at 3000 rpm. A small aliquot of the emulsion phase was taken and plunged in liquid nitrogen followed by fracture at -130 °C using a flat edge cold knife. The surface solvent was sublimed at -95 °C for 5 min. The sample was sputtered with a gold-palladium composite at 10 mA for 88 s and imaged using a Hitachi S-4800 Field Emission SEM operated at a voltage of 3 kV and a working distance of ~9 mm.

**2.6. Rheological Studies and Zeta Potential Measurements.** Steady-shear rheological measurements were made at 25 °C on a TA Instruments AR 2000 rheometer using a cone and plate geometry of 40 mm diameter with 1° cone angle. The zeta potential of the emulsion samples of crude oil in saline water was determined by measuring the electrophoretic mobility of the droplets using Laser Doppler Velocimetry (Zetasizer Nano, Malvern Instruments). The emulsion samples were prepared using Corexit with a dispersant to oil volume ratio of 0.05. LHMC was added in varying LHMC to Corexit mass ratios. The pH of the emulsions was adjusted and maintained at 4 by adding 1% acetic acid solution. The emulsions were stirred for 1 min on a vortex mixer operating at 3000 rpm. Approximately 1 mL of the emulsion phase was transferred to a polypropylene electrode cell, and the zeta potential was measured following a temperature equilibration at 25 °C for 2 min.

### 3. RESULTS AND DISCUSSION

**3.1. Interfacial Tension.** The reduction of interfacial tension between crude oil and water is a key factor in the creation of smaller oil droplets and their entrainment into the water column.<sup>2</sup> The interfacial tension between crude oil and water depends on the composition of oil and is greatly

influenced by weathering factors.<sup>1,2</sup> In our studies, we used Louisiana sweet crude oil collected from the Macondo prospect in the Gulf of Mexico, with a viscosity of ~0.01 Pa s at 15 °C, and specific gravity ~0.85 at 15 °C.<sup>32</sup> The measured interfacial tension between crude oil and saline water is 24.6 ± 1.1 mN/m. Figure 2 shows the effect of the dispersant level on the

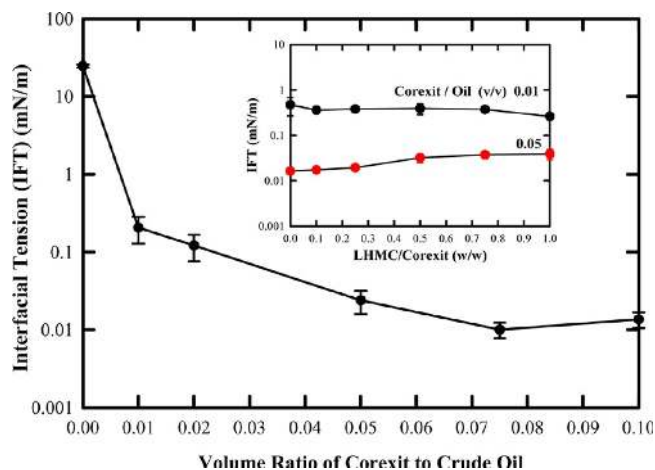


**Figure 2.** Effect of the amount of dispersant expressed as the volume ratio of Corexit to crude oil on the interfacial tension between crude oil and saline water. The inset shows the effect of the mass ratio of LHMC to Corexit on the interfacial tension between crude oil and saline water for two different dispersant to oil volume ratios (0.01 and 0.05).

interfacial tension between crude oil and saline water. The addition of Corexit reduces the interfacial tension significantly with a decrease of 2 orders of magnitude for a low dispersant to oil volume ratio of 0.01. We have done experiments where the dispersant was first introduced into the oil droplet before mixing with water, since the presence of light hydrocarbon distillates as a solvent allows solubility in the oil phase. The equilibrium interfacial tensions measured (Supporting Information, Figure S-2) are within the statistical error of results reported in Figure 2 when the dispersant is added to the water phase first. The results imply that the dispersant originally designed for aerial delivery in the treatment of surface spills is also effective when applied in deep sea environments if applied sufficiently close to the oil release, if the surfactants in the dispersants are able to rapidly partition to the oil-water interface.<sup>2</sup>

The inset to Figure 2 shows the effect of addition of LHMC on the reduced interfacial tension between crude oil and saline water due to Corexit. The dispersant was added to the oil phase, and LHMC was added to the aqueous phase. For both surfactant levels (dispersant to oil volume ratios of 0.05 and 0.01), the addition of LHMC does not cause a significant change in the interfacial tension. In the absence of Corexit, LHMC has negligible impact on the equilibrium interfacial tension between crude oil and saline water. The measurements using the pendant drop method (Supporting Information, Figure S-3) indicate that for low concentrations of LHMC, the reduction in the interfacial tensions between crude oil and saline water is insignificant within the statistical error. These observations are in accordance with earlier observations that chitosan has negligible surface activity.<sup>33,34</sup>

**3.2. Emulsion Stability and Characterization.** To study the influence of the biopolymer on the dispersant effectiveness,



Corexit was first mixed with crude oil with a dispersant to oil volume ratio of 0.01 and then added to two vials containing saline water. The oil to water ratio was maintained at 0.01. An acidic solution of LHMC was added to one of the vials with a mass ratio of LHMC to Corexit of 0.5. The vials were stirred together for 30 s at 3000 rpm and then left undisturbed. Figure 3a shows photographs of the vials taken at regular intervals after cessation of stirring. The control sample without HMC (top row, Figure 3a) indicates a very rapid coalescence of oil droplets even within the time frame of starting the experiment, as evidenced by the rapid formation of the ring of oil at the air water interface. Within 30 min it is clear that much of the turbidity in solution has been lost. The vial containing LHMC in addition to the dispersant (bottom row, Figure 3a) shows a significant delay in the coalescence of oil droplets and retains a significant turbidity even after 30 min. This experiment gives visual evidence of the ability of LHMC to enhance the dispersion capability of Corexit. We have also performed experiments with seawater (pH 7.9, conductivity 85 mS/cm) collected from the Gulf of Mexico and see a similar observation where the addition of LHMC significantly delays the coalescence of crude oil droplets (Supporting Information, Figure S-4). We propose that the stabilization is the result of LHMC anchoring to oil droplets that have been formed through the addition of Corexit to oil, and stabilizing the droplets through a combination of steric and electrostatic repulsion.

Imaging of the droplets was then done through optical microscopy (Nikon Eclipse LV100 fitted with a digital camera), with samples of the aqueous phase from the vials taken both immediately and 30 min after stirring was stopped. A small aliquot of the aqueous phase containing dispersed oil was placed on a glass slide and covered with a glass coverslip. Figure 3b-A is the optical microscope image of the sample where crude oil was dispersed with the aid of only Corexit. The aqueous bottom phase contained both bigger droplets ( $\sim 100 \mu\text{m}$ ) and smaller droplets ( $\sim 20 \mu\text{m}$ ) immediately after stirring, with rapid coalescence leading to blurring of the image. It was observed that the bigger oil droplets were unstable and coalesced quickly and moved to the edges of the coverslip. For the bulk aqueous phase sample collected 30 min past the stirring (Figure 3b-B), only very small uncoalesced droplets were observed, with most of the oil having formed the surface ring shown in Figure (3a, top right).

Figure (3b-C) shows the optical microscopy image of the aqueous phase in the sample containing LHMC. Oil droplets with a wide size range ( $10\text{--}100 \mu\text{m}$ ) were observed in the aqueous phase immediately after stirring. When compared to the emulsion dispersed using Corexit alone, the droplets were observed to be significantly more stable. Thirty minutes after cessation of stirring, the aqueous phase still contained oil droplets with a wide size distribution (Figure 3b-D). There is qualitative evidence of some coalescence as the distribution seems to have shifted slightly to larger droplet size, but with retention of colloidal stability in the aqueous phase.

Turbidimetric measurements of the aqueous phase containing crude oil dispersed with the aid of Corexit are shown in Figure 4a. For the control sample, where no dispersant was used, the transmittance steeply increases to 80% within the initial few minutes and then steadily increases to 95% indicating that most of the oil droplets separate from the aqueous phase quickly and come to the surface. For the dispersant to oil ratio of 0.001, the addition of Corexit does not indicate a significant

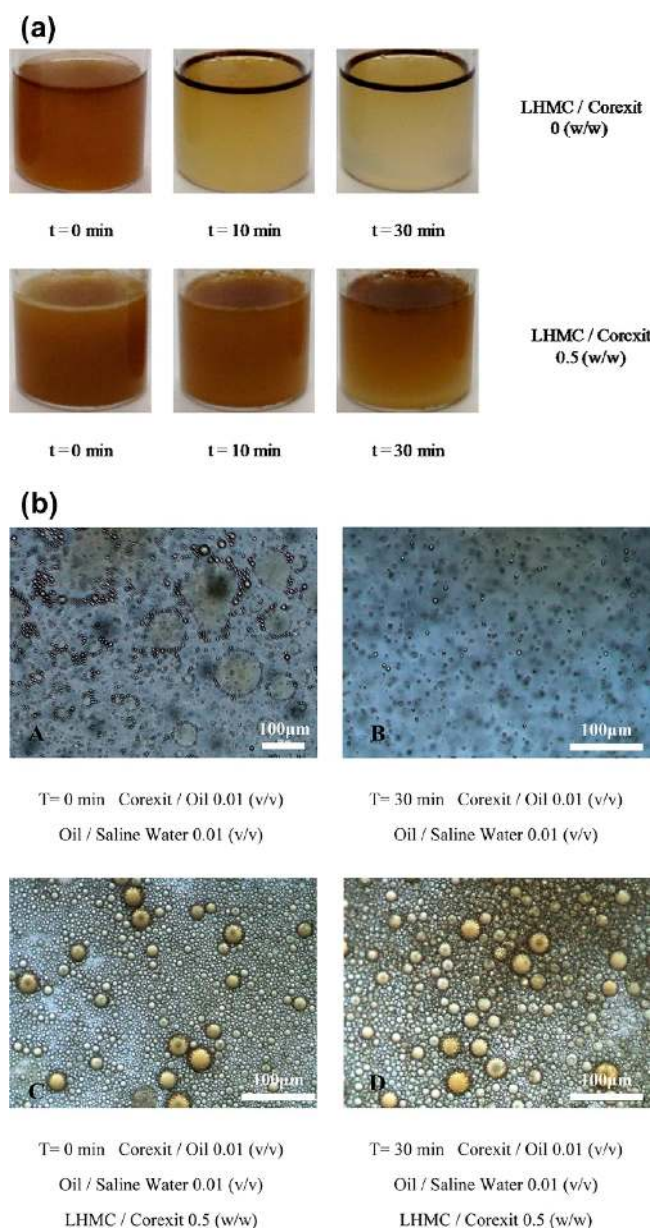


**Figure 3.** (a) Photographic images showing the increased stability of the crude oil droplets in the aqueous phase upon the addition of LHMC. The volume ratio of Corexit to crude oil was 0.01. The mass ratio of LHMC to Corexit is 0.5 in the sample shown in the bottom row. Both samples were stirred together for 30 s at 3000 rpm and then left undisturbed on the counter. The vial containing both Corexit and LHMC (bottom row) has more oil dispersed in the aqueous phase after 30 min in comparison with the vial containing only Corexit (top row). (b) Optical microscopy images of crude oil droplets dispersed in saline water using Corexit with the dispersant to oil volume ratio of 0.01 without LHMC (A and B) and with LHMC (C and D). The mass ratio of LHMC to Corexit was 0.5. The vials were stirred together for 30 s at 3000 rpm and then left undisturbed on the counter. The large droplets in the sample without LHMC coalesced over the period of 30 min, leaving only smaller droplets in the aqueous phase (B). The droplets stabilized by LHMC (D) were more stable over the period of 30 min.

difference in the transmittance versus time curve from the control. In the case, where the dispersant to oil volume ratio is 0.01 and greater, the system retains turbidity for extended periods as indicated by the low transmittance values that persist

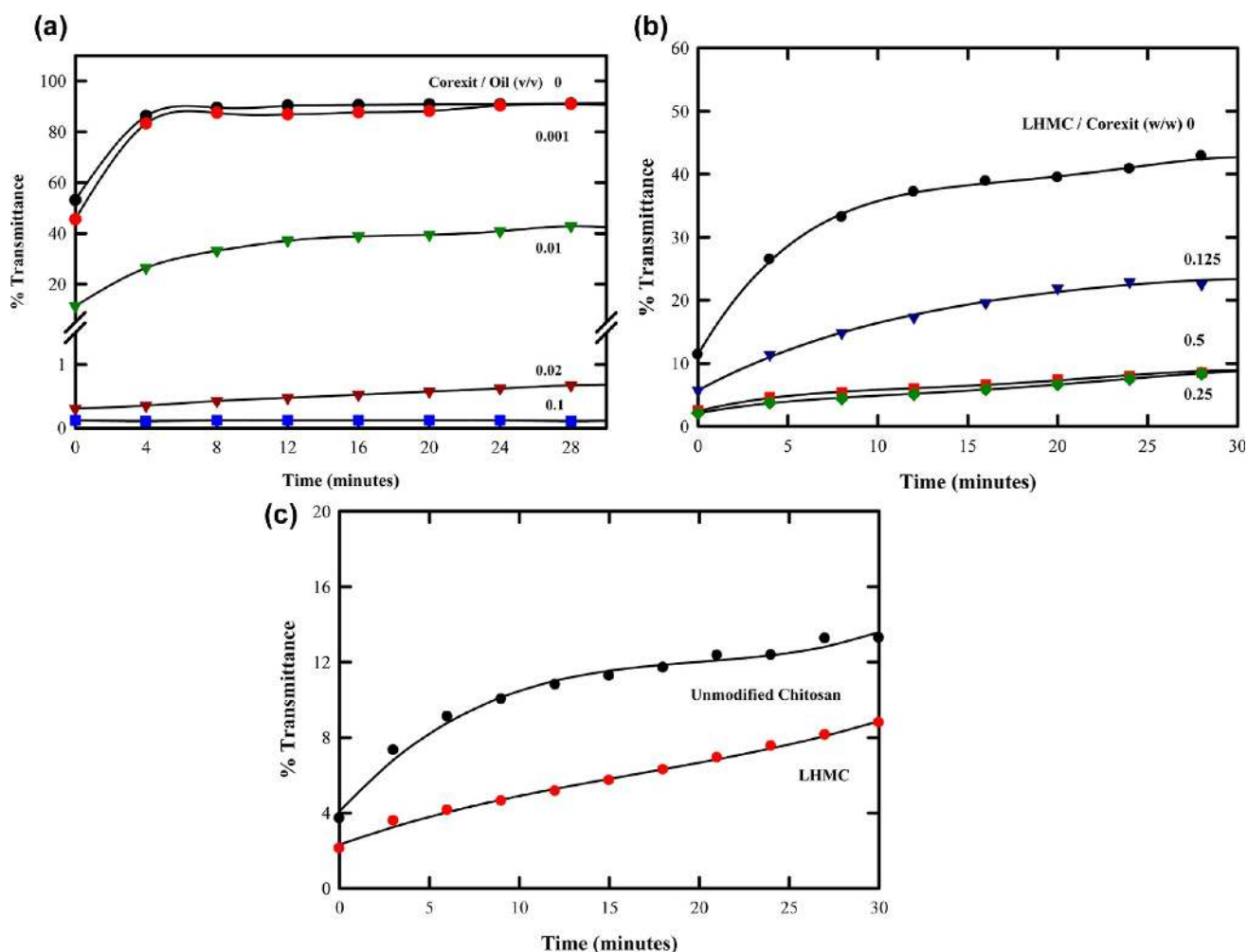


**Figure 4.** (a) Increase in the dispersant to oil volume ratio increases the stability of the crude oil-in-saline water emulsion. The crude oil to saline water volume ratio was maintained as 0.003. (b) Effect of the mass ratio of LHMC to Corexit on the stability of crude oil-in-saline water emulsions. The dispersant to oil volume ratio was 0.01. The crude oil to saline water volume ratio was maintained as 0.003. The addition of LHMC enhances the stability of the dispersed oil droplets resulting in the increased turbidity of the aqueous phase. (c) Effect of hydrophobic modification of chitosan on the stability of the crude oil-in-saline water emulsion prepared using the combination of Corexit and chitosan. The dispersant to oil volume ratio was 0.01. The crude oil to saline water volume ratio was maintained as 0.003. For the same mass ratio of polymer to Corexit (0.25), LHMC stabilized the oil droplets more efficiently than unmodified chitosan.

for over 30 min. We have used a value of 0.01 for the dispersant to oil ratio in succeeding experiments where the effect of LHMC is characterized. Figure 4b shows the effects of adding varying amounts of LHMC as defined as the mass ratio of LHMC to Corexit. There is clearly an improvement in maintaining the dispersion. At LHMC to Corexit ratios of 0.25 and higher, the system shows considerable stability for extended time periods exceeding 30 min, although there is a negligible improvement in stability beyond a ratio of 0.25. The turbidimetric measurements are consistent with the visual observations and indicate that small amounts of LHMC can significantly improve the stability of the dispersed oil droplets.

To further understand the stabilizing effect of LHMC, we compared the dispersion characterization of drops stabilized with LHMC with those stabilized by unmodified chitosan (UC). Figure 4c illustrates the results of the comparison done for a chitosan to Corexit ratio of 0.25 (w/w). It is observed that unmodified chitosan also enhances the stability of the droplets although it is not as effective as LHMC. While the cationic chitosan would be expected to interact with the anionic DOSS of Corexit, thus positioning itself at the oil–water interface, our

explanation of the additional stabilization is the anchoring of the hydrophobic alkyl groups of LHMC to oil droplets, forming a coating over the drops.

The steady shear viscosities of the aqueous phase containing crude oil dispersed by Corexit and stabilized by LHMC are shown in Figure 5. For the case where the mass ratio of LHMC to Corexit is 10, the viscosity of the aqueous phase was not observed to be significantly different from the viscosity of saline water. Increasing the mass ratio of LHMC to Corexit from 10 to 50 results in an increase of the viscosity of the aqueous phase from 0.0015 Pa s to 0.004 Pa s. The mass ratios of LHMC to Corexit used in the turbidimetric studies were 0.25 or lower confirming that the addition of small amounts of LHMC does not impact the viscosity of the aqueous phase. This further supports our hypothesis that the delay in the coalescence of the oil droplets in the aqueous phase is due to the adsorption of the biopolymer at the oil–water interface and not due to the viscosity of the aqueous phase.

Table 1 shows the effect of LHMC on the zeta potential of crude oil droplets dispersed in saline water and deionized water using Corexit. For the control sample, where no LHMC was

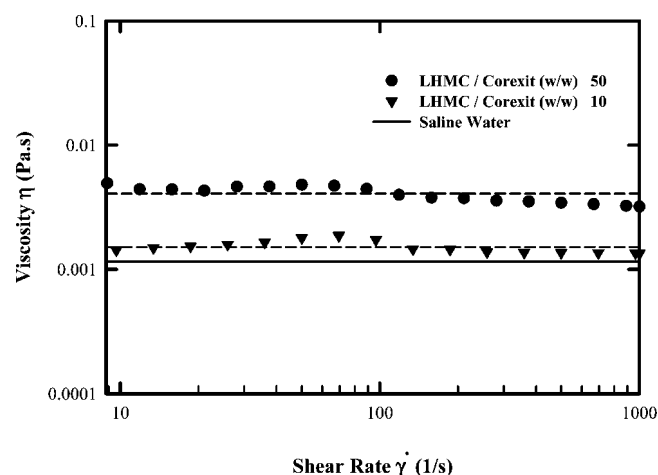


**Figure 5.** Steady shear viscosity measurement of crude oil-in-saline water emulsion prepared using Corexit and LHM for oil to saline water volume ratio of 0.01. The addition of LHM has no significant effect on the viscosity of the emulsion at low mass ratios of LHM to Corexit.

**Table 1.** Effect of LHM on the Zeta Potential of Crude Oil-in-Water Emulsion Stabilized by Corexit

mass ratio of LHM to Corexit	zeta potential (mV)	
	NaCl conc. (0.6 M) pH = 4.0	NaCl conc. (0 M) pH = 4.0
0.000	$-3.88 \pm 2.83$	$-52.53 \pm 2.40$
0.063	$6.87 \pm 2.89$	$38.27 \pm 1.01$
0.125	$11.08 \pm 1.44$	$44.71 \pm 3.18$
0.250	$10.68 \pm 0.91$	$50.77 \pm 3.48$
0.500	$11.37 \pm 0.93$	$43.52 \pm 1.14$
1.000	$11.12 \pm 3.64$	$42.13 \pm 2.30$

added, the zeta potential of the crude oil droplets was measured as  $-4$  mV in saline water (0.6 M NaCl) and  $-53$  mV in deionized water. The negative charge of the oil droplets is due to the anionic DOSS present in Corexit. The low value of the zeta potential of oil droplets in saline water is due to the electrostatic screening effect of  $\text{Na}^+$  ions.<sup>12,35</sup> In saline water, the addition of a small amount of LHM at an LHM to Corexit mass ratio of 0.063 results in the reversal of charge on the oil droplet with a positive zeta potential of 7 mV. Increasing the mass ratio of LHM to Corexit from 0.063 to 0.125 increases the zeta potential to 11 mV. No significant increase in the zeta potential of the oil droplets was observed with a further increase in the concentration of LHM. These results further corroborate our hypothesis that the cationic LHM adsorbs at the oil–water interface. Once the surface of an oil droplet is saturated with the polysaccharide chains, further addition of the LHM does not result in any further increase in the electrostatic repulsion to coalescence.<sup>20</sup> The effect of LHM on the surface charge of oil droplets is more pronounced in deionized water, where the zeta potential of the oil droplets changed from negative to positive reaching a relatively constant value ( $\approx +50$  mV) with increase in LHM concentration.<sup>20</sup>

High resolution cryo-SEM images of the aqueous phase are shown in Figure 6. The panels on the left show oil droplets dispersed in saline water with the aid of Corexit at increasingly higher resolution (Figure 6A–C), while those on the right show droplets in the presence of Corexit and LHM (Figure 6D–F). The relatively high mass ratio of HMC to Corexit of

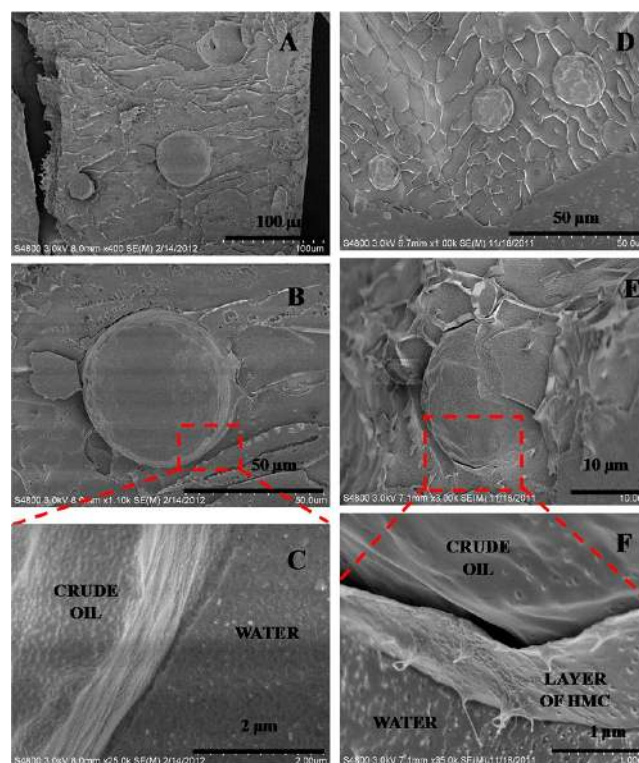


**Figure 6.** High resolution cryogenic Scanning Electron Microscope (cryo-SEM) images of oil droplet dispersed by Corexit (A–C) and after sequential addition of LHM (D–F). A layer of polymer around the oil droplet is observed in the sample containing LHM (F). Dispersant to oil volume ratio of 0.01 was used in both of the samples. The mass ratio of LHM to Corexit is unity.

unity was used to visualize the presence of the polymer layer around the oil droplet. As shown in Figure 6, the interface between the crude oil and the water containing only Corexit is smooth (Figure 6C). The presence of LHM at the oil–water interface can be clearly seen in the sample stabilized by addition of the biopolymer (Figure 6F). This is direct evidence for the adsorption of the polymer at the oil–water interface. The layer of biopolymer around the oil droplet seen in the high resolution cryo SEM images confirms our hypothesis that low molecular mass HMC adsorbs at the crude-oil–water interface. We speculate that the adsorbed polymer enhances the colloidal stability of the dispersed oil droplets by increasing the electrostatic repulsions and also by providing a steric barrier to coalescence.

**3.3. Effects of High Molecular Weight Hydrophobically Modified Chitosan (HHMC).** The use of high molecular weight HMC (HHMC) brings about the phenomenon where the polymer bridges between oil droplets. Figure 7a shows the steady shear viscosities of the aqueous phase containing crude oil dispersed by Corexit into emulsion droplets. The droplets are then treated with LHM and HHMC, and the steady state viscosities are measured. The dispersant to oil volume ratio and the mass ratio of HMC to Corexit were kept constant in both samples. The viscosity of the sample stabilized by the HHMC is an order of magnitude greater than the viscosity of the sample stabilized by LHM. Measurements of the elastic and viscous moduli of these systems show additional differences in the rheological properties (Figure 7b). For the sample containing LHM, the elastic modulus ( $G'$ ) is lower than its viscous modulus ( $G''$ ) at lower oscillation frequencies. A crossover at



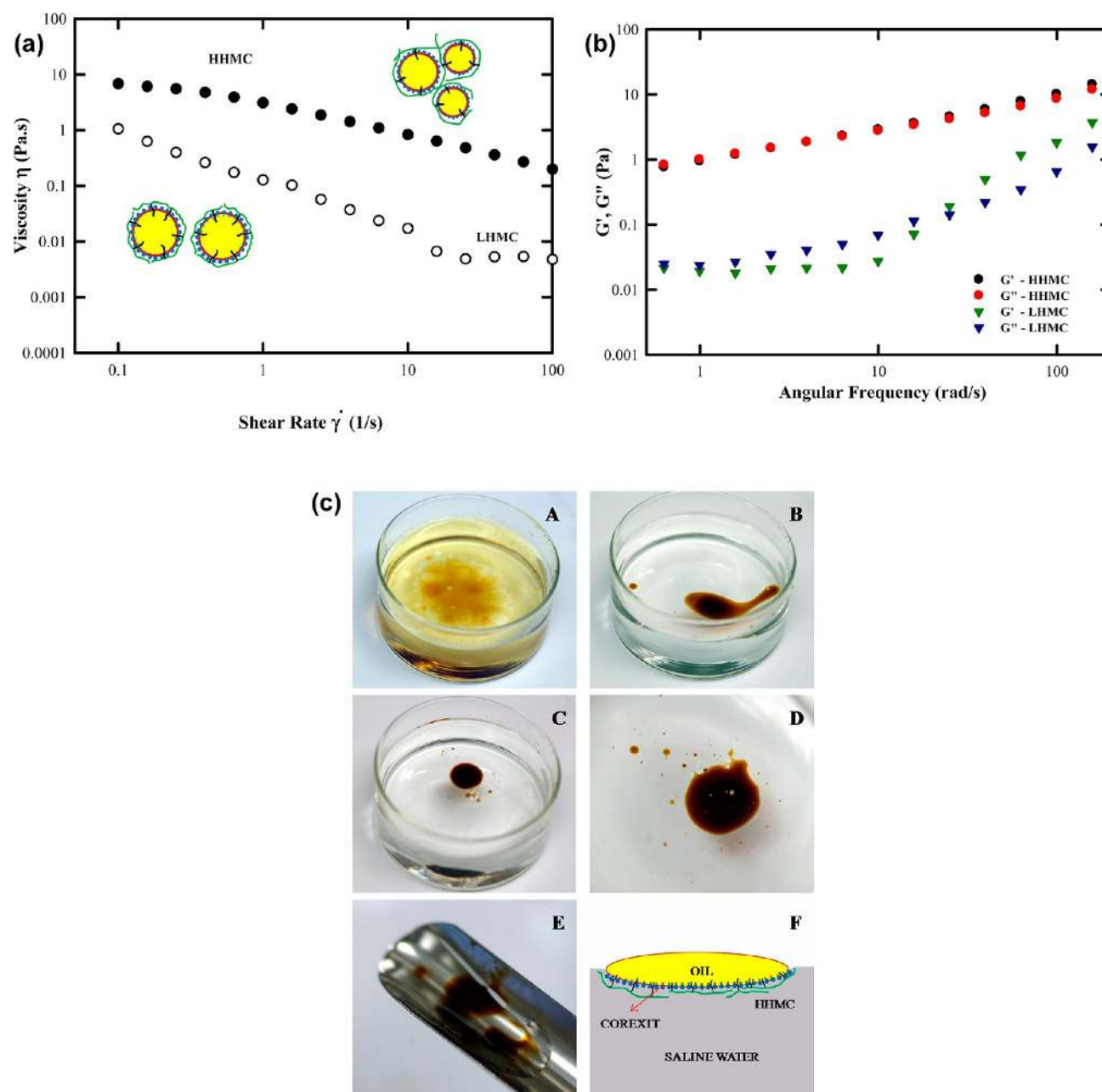


**Figure 7.** (a) Effect of the molecular weight of HMC on the viscosity of crude oil-in-saline water emulsions prepared using Corexit and HMC for high volume ratio of crude oil to saline water (0.1). The dispersant to oil volume ratio was 0.01 and HMC to Corexit mass ratio was 10. The viscosity of the emulsion stabilized by HHMC is orders of magnitude greater than that of the emulsion stabilized by LHMC. The increase in the viscosity is due to the ability of the high molecular weight biopolymer to span oil droplets with hydrophobic residues anchored at the oil–water interface. (b) Elastic ( $G'$ ) and viscous ( $G''$ ) modulus of the emulsion of crude oil-in-saline water emulsion prepared using Corexit and HMC for high volume ratio of crude oil to saline water (0.1). The dispersant to oil volume ratio was 0.01 and HMC to Corexit mass ratio was 10. While the emulsion stabilized by LHMC shows characteristics of a viscous solution, the emulsion stabilized by HHMC behaves like a very weak gel. (c) Experiment demonstrating the ability of HHMC to bind the oil corralled from a surface spill using Corexit. (A) A layer of crude oil on the surface of saline water. (B) Application of Corexit along the edge thickens the slick. (C) Application of HHMC results in the formation of a gel-like aggregate. (D) A close-up image of the gel-like phase containing crude oil that can be collected using a spatula (E). (F) Schematic showing crude oil corralled by Corexit and bound by HHMC in a gel-like aggregate.

higher frequencies is observed when the value of  $G'$  becomes greater than  $G''$ , characteristic of a viscous fluid.<sup>36,37</sup> In the case of HHMC, the values of  $G'$  and  $G''$  are similar and  $G'$  is slightly greater than  $G''$  over the range of frequency sweep. This indicates a transition from a viscous solution to a weak gel.<sup>36,37</sup> We speculate that at higher concentrations and high molecular weights, the long polymer chains form a gel-like matrix with the

hydrophobic residues anchored at the oil–water interface. These observations agree with previous studies where HMC is able to gel hydrophobic moieties such as carbon microspheres and vesicles.<sup>28,29</sup>

To demonstrate the ability of HHMC to bind the oil in a gel-like phase, 100  $\mu\text{L}$  of crude oil was allowed to form a film on the surface of saline water in a Petri dish (Figure 7c-A).

Application of Corexit (dispersant to oil volume ratio 0.01) along the edges of the Petri dish results in corralling of the crude oil film by surfactant molecules due to Marangoni effects of introducing surface convective flow due to surface tension gradients and subsequent thickening of the oil layer (Figure 7c-B). Application of HHMC (mass ratio of HHMC to crude oil = 0.05) results in the formation of a highly viscous phase containing crude oil (Figure 7c-C and Figure 7c-D) which can be collected using a spatula (Figure 7c-E). In the absence of HHMC addition, this oil layer cannot be picked up and breaks up when collection is attempted. The results point to methods of immobilizing small surface spills for ease in removal through skimming. We propose that the synergistic approach of using Corexit and HHMC to thicken the oil using HHMC may find application in oil spill collection in calm waters when wave energy is insufficient to break up spills into dispersed droplets.

#### 4. CONCLUSIONS

Sequential application of low molecular weight hydrophobically modified chitosan (LHMC) significantly enhances the stability of crude oil droplets dispersed in saline water by Corexit because of the adsorption of the cationic biopolymer at the oil–water interface. The formation of a protective polymer layer around the oil droplet enhances colloidal stability by increasing the electro-steric repulsion between oil droplets. The attachment of LHMC at the oil–water interface is driven by hydrophobic interactions resulting in the anchoring of alkyl groups. At low volume ratios of oil to water, as is the case in oil spills, the addition of LHMC at the low concentrations used to stabilize droplets does not modify viscosity of the aqueous phase. These results obtained with saline water can be extended to experiments in seawater (Supporting Information, Figure S-4) and present potential for field applications. An increase in the molecular weight of HMC (HHMC) results in an increase in the viscosity which we propose is due to the tethering of oil droplets by HHMC, resulting in the formation of gel like aggregates. When HHMC is applied to surface sheens of oil, it thickens the oil through such tethering of droplets.

Two potential scenarios for the application of HMC in oil spill remediation are therefore presented in this paper:

(a) Application of low molecular weight HMC (LHMC) can significantly enhance the stability of crude oil droplets dispersed through the use of chemical dispersants such as Corexit 9500. The results from our study point to potentially minimizing the use of chemical dispersants in the case of large spills such as from the Deepwater Horizon Spill, through the use of hydrophobically modified polysaccharides for enhanced stability and bacterial remediation of dispersed oil. In practical application, LHMC can be applied to a spill aerially or at the wellhead in dilute acidic media. When delivered directly to the oil phase, the polymer is expected to anchor at the interface.

(b) The application of high molecular weight HMC (HHMC) can increase the viscosity of the dispersed phase significantly through increased cross-linking and tethering of oil droplets. We demonstrate that the subsequent application of dispersant and HHMC can corral and immobilize oil for the ease of removal by mechanical means. These results could be extended to the remediation of smaller spills such as from a barge or oil-tanker

Chitosan and its derivatives are considered nontoxic<sup>38</sup> and biocompatible.<sup>15,39</sup> However, the possible cytotoxicity of chitosan on aquatic biota because of its cationic nature needs further investigation. The concept of enhancing the stability of

dispersed crude oil droplets by the hydrophobically modified polysaccharides can be extended to other natural polymers such as the alginates<sup>40,41</sup> which are anionic, and will be pursued in continuing research. The oceans contain significant amount of polysaccharides known as exopolymers, albeit in very dilute levels.<sup>42</sup> The harvesting of these entirely innocuous biopolymers for spill remediation is a significant technological possibility. The ability of modified polysaccharides to non-covalently bind with vesicles and biological cells<sup>17,28</sup> and stabilize oil-in-water emulsions<sup>22</sup> could result in an enhanced bioremediation of spills.

The implications of our results to current remediation methods are significant in the view of potentially reducing dispersant (synthetic surfactant + hydrocarbon solvent) use and substituting biopolymers. Such synergistic effects of modified natural biopolymers and dispersants for oil spill remediation could result in a novel environmentally benign and effective marine oil spill remediation technology for treating future oil seeps and spills.

#### ■ ASSOCIATED CONTENT

##### Supporting Information

This section includes information on the structure and <sup>1</sup>H NMR spectra of HMC, the effect of the amount of dispersant (Corexit) on the interfacial tension between crude oil and saline water when the dispersant is applied to the oil phase (Figure S-2), effect of LHMC on the interfacial tension between crude oil and saline water (Figure S-3) and visual demonstration of increased stability of dispersed crude oil droplet in seawater (pH 7.9) (Figure S-4). This material is available free of charge via the Internet at <http://pubs.acs.org>.

#### ■ AUTHOR INFORMATION

##### Corresponding Author

\*Phone: 504-865-5883. Fax: 504-865-6744. E-mail: [vj@tulane.edu](mailto:vj@tulane.edu).

##### Notes

The authors declare no competing financial interest.

#### ■ ACKNOWLEDGMENTS

Support from the National Science Foundation (Grant 1049330) and the Gulf of Mexico Research Initiative is gratefully acknowledged.

#### ■ REFERENCES

- (1) Fingas, M. In *Oil Spill Science and Technology*; Mervin, F., Ed.; Gulf Professional Publishing: Boston, MA, 2011; pp 435–582.
- (2) *Oil Spill Dispersants: Efficacy and Effects*; National Research Council: Washington, DC, 2005.
- (3) Thibodeaux, L. J.; Valsaraj, K. T.; John, V. T.; Papadopoulos, K. D.; Pratt, L. R.; Pesika, N. S. *Environ. Eng. Sci.* **2011**, *28*, 87–93.
- (4) George-Ares, A.; Clark, J. R. *Chemosphere* **2000**, *40*, 897–906.
- (5) Steffy, D.; Nichols, A.; Kiplagat, G. *Ocean Sci. J.* **2011**, *46*, 299–305.
- (6) Mukherjee, B.; Wrenn, B. A. *Environ. Eng. Sci.* **2011**, *28*, 263–273.
- (7) Kujawinski, E. B.; Soule, M. C. K.; Valentine, D. L.; Boysen, A. K.; Longnecker, K.; Redmond, M. C. *Environ. Sci. Technol.* **2011**, *45*, 1298–1306.
- (8) Li, Z. K.; Lee, K.; King, T.; Kepkay, P.; Boufadel, M. C.; Venosa, A. D. *Environ. Eng. Sci.* **2009**, *26*, 1139–1148.
- (9) Li, Z. K.; Lee, K.; King, T.; Boufadel, M. C.; Venosa, A. D. *Environ. Eng. Sci.* **2009**, *26*, 1407–1418.



- (10) Belore, R. C.; Trudel, K.; Mullin, J. V.; Guarino, A. *Mar. Pollut. Bull.* **2009**, *58*, 118–128.
- (11) Moles, A.; Holland, L.; Short, J. *Spill Sci. Technol. Bull.* **2002**, *7*, 241–247.
- (12) Sterling, M. C.; Bonner, J. S.; Ernest, A. N. S.; Page, C. A.; Autenrieth, R. L. *Mar. Pollut. Bull.* **2004**, *48*, 969–977.
- (13) Rinaudo, M. *Prog. Polym. Sci.* **2006**, *31*, 603–632.
- (14) Ravi Kumar, M. N. V. *React. Funct. Polym.* **2000**, *46*, 1–27.
- (15) Kean, T.; Thanou, M. *Adv. Drug Delivery Rev.* **2010**, *62*, 3–11.
- (16) Sashiwa, H.; Aiba, S.-i. *Prog. Polym. Sci.* **2004**, *29*, 887–908.
- (17) Dowling, M. B.; Kumar, R.; Keibler, M. A.; Hess, J. R.; Bochicchio, G. V.; Raghavan, S. R. *Biomaterials* **2011**, *32*, 3351–3357.
- (18) Francis Suh, J. K.; Matthew, H. W. T. *Biomaterials* **2000**, *21*, 2589–2598.
- (19) Guzey, D.; McClements, D. J. *Adv. Colloid Interface Sci.* **2006**, *128*, 227–248.
- (20) Mun, S.; Decker, E. A.; McClements, D. J. *Langmuir* **2005**, *21*, 6228–6234.
- (21) Bratskaya, S.; Avramenko, V.; Schwarz, S.; Philippova, I. *Colloids Surf., A* **2006**, *275*, 168–176.
- (22) Wongkongkatep, P.; Manopwisedjaroen, K.; Tiposoth, P.; Archakunakorn, S.; Pongtharangkul, T.; Suphantharika, M.; Honda, K.; Hamachi, I.; Wongkongkatep, J. *Langmuir* **2012**, *28*, 5729–5736.
- (23) Rodríguez, M. S.; Albertengo, L. A.; Agulló, E. *Carbohydr. Polym.* **2002**, *48*, 271–276.
- (24) Schulz, P. C.; Rodríguez, M. S.; Del Blanco, L. F.; Pistonesi, M.; Agullo, E. *Colloid Polym. Sci.* **1998**, *276*, 1159–1165.
- (25) Del Blanco, L. F.; Rodríguez, M. S.; Schulz, P. C.; Agullo, E. *Colloid Polym. Sci.* **1999**, *277*, 1087–1092.
- (26) Desbrieres, J.; Babak, V. *Soft Matter* **2010**, *6*, 2358–2363.
- (27) Desbrieres, J.; Martinez, C.; Rinaudo, M. *Int. J. Biol. Macromol.* **1996**, *19*, 21–28.
- (28) Lee, J. H.; Gustin, J. P.; Chen, T. H.; Payne, G. F.; Raghavan, S. R. *Langmuir* **2005**, *21*, 26–33.
- (29) St Dennis, J. E.; Meng, Q. K.; Zheng, R. N.; Pesika, N. S.; McPherson, G. L.; He, J. B.; Ashbaugh, H. S.; John, V. T.; Dowling, M. B.; Raghavan, S. R. *Soft Matter* **2011**, *7*, 4170–4173.
- (30) Vonnegut, B. *Rev. Sci. Instrum.* **1942**, *13*, 6–9.
- (31) Zattoni, A.; Loli Piccolomini, E.; Torsi, G.; Reschiglian, P. *Anal. Chem.* **2003**, *75*, 6469–6477.
- (32) Wang, Z.; Hollebone, B. P.; Fingas, M.; Fieldhouse, B.; Sigouin, L.; Landriault, M.; Smith, P.; Noonan, J.; Thouin, G.; Weaver, J. J. *Characteristics of Spilled Oils, Fuels, and Petroleum Products: 1. Compositions and Properties of Selected Oils*; United States Environmental Protection Agency: Research Triangle Park, NC, 2003.
- (33) Babak, V.; Lukina, I.; Vikhoreva, G.; Desbrieres, J.; Rinaudo, M. *Colloids Surf., A* **1999**, *147*, 139–148.
- (34) Babak, V. G.; Desbrieres, J. *Colloid Polym. Sci.* **2006**, *284*, 745–754.
- (35) Klinkesorn, U.; Namatsila, Y. *Food Hydrocolloids* **2009**, *23*, 1374–1380.
- (36) Raghavan, S. R.; Riley, M. W.; Fedkiw, P. S.; Khan, S. A. *Chem. Mater.* **1998**, *10*, 244–251.
- (37) Macosko, C. W. *Rheology: Principles, Measurements and Applications*; Wiley-VCH: New York, 1994.
- (38) McClements, D. J.; Decker, E. A.; Weiss, J. J. *Food Sci.* **2007**, *72*, R109–R124.
- (39) Boesel, L. F.; Reis, R. L.; Roman, J. S. *Biomacromolecules* **2009**, *10*, 465–470.
- (40) Bu, H. T.; Nguyen, G. T. M.; Kjoniksen, A. L. *Polym. Bull.* **2006**, *57*, 563–574.
- (41) Pawar, S. N.; Edgar, K. J. *Biomaterials* **2012**, *33*, 3279–3305.
- (42) Bar-Zeev, E.; Berman-Frank, I.; Liberman, B.; Rahav, E.; Passow, U.; Berman, T. *Desalin. Water Treat.* **2009**, *3*, 136–142.

## Supporting Information

**Attachment of a Hydrophobically Modified Biopolymer at the Oil-Water Interface in the Treatment of Oil Spills**

Pradeep Venkataraman<sup>1</sup>, Jingjian Tang<sup>1</sup>, Etham Frenkel<sup>1</sup>, Gary L. McPherson<sup>2</sup>, Jibao He<sup>3</sup>, Srinivasa R. Raghavan<sup>4</sup>, Vladimir Kolesnichenko<sup>5</sup>, Arijit Bose<sup>6</sup>, Vijay T. John<sup>1\*</sup>

1. Department of Chemical and Biomolecular Engineering  
Tulane University, New Orleans, LA 70118  
Email: vj@tulane.edu. Phone: (504) 865-5883. Fax: (504) 865-6744
2. Department of Chemistry  
Tulane University, New Orleans, LA 70118
3. Coordinated Instrumentation Facility  
Tulane University, New Orleans, LA 70118
4. Department of Chemical and Biomolecular Engineering  
University of Maryland, College Park, MD 20742
5. Department of Chemistry  
Xavier University of Louisiana, New Orleans, LA 70125
6. Department of Chemical Engineering  
University of Rhode Island, Kingston, RI 02881

\*Corresponding author. Phone: 504-865-5883. E-mail: vj@tulane.edu.

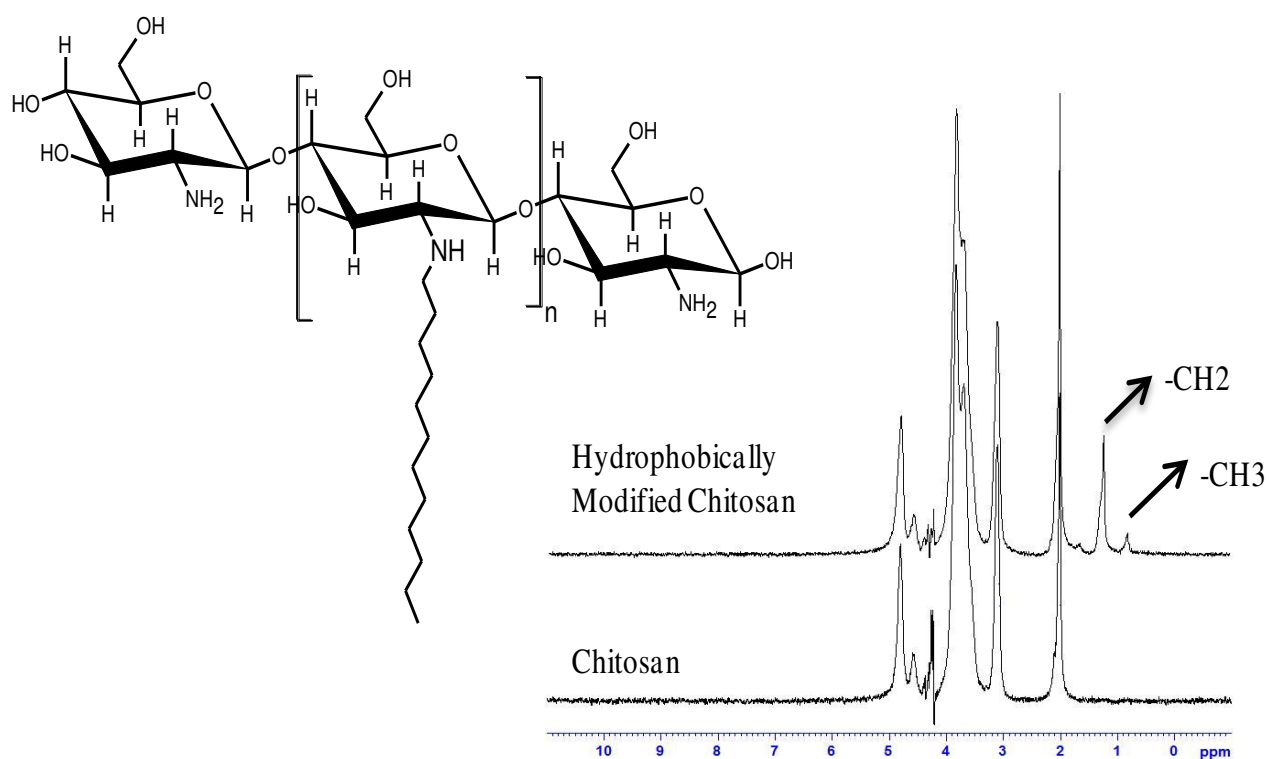


**Figure S-1.** Structure of hydrophobically modified chitosan molecule. 2.5% of the glucosamine monomers on the polymer chain were hydrophobically modified by covalently attaching n-dodecyl tails.  $^1\text{H}$  NMR spectrum showing the peaks for the alkyl residues attached to the chitosan polymer backbone.



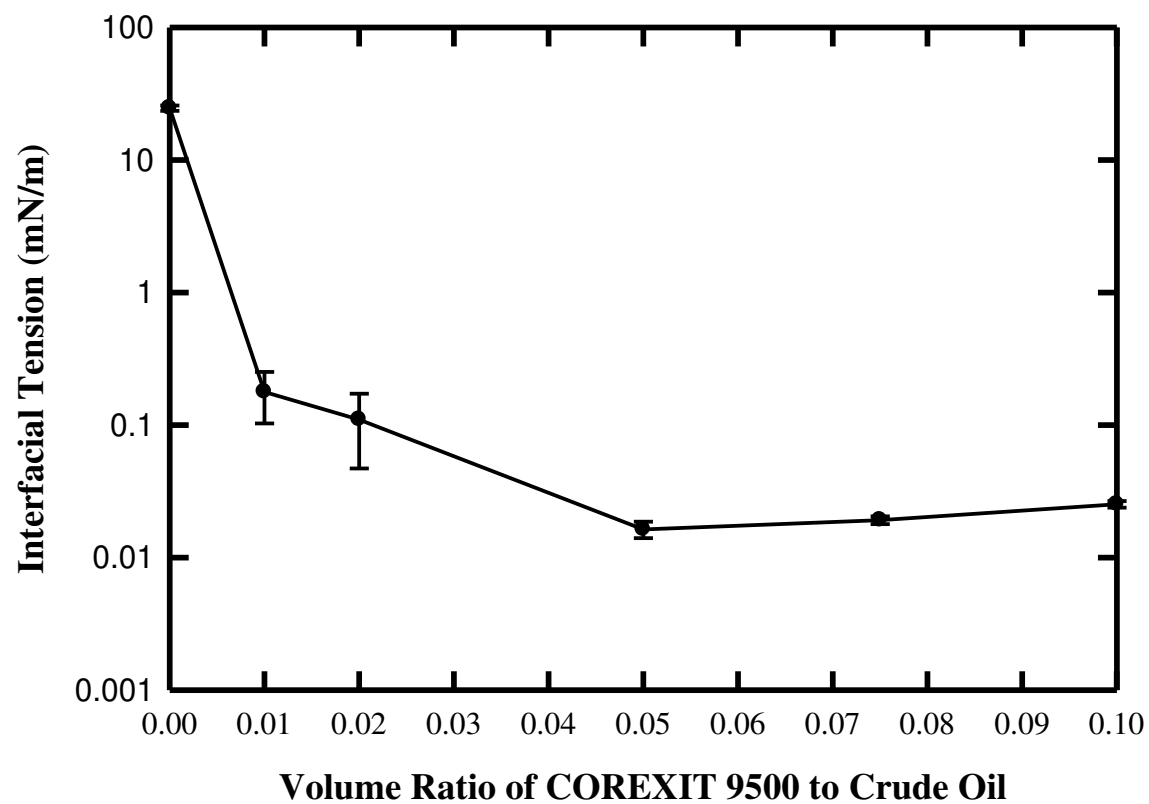


**Figure S-2.** Effect of the amount of dispersant (expressed as the volume ratio of Corexit to crude oil) on the interfacial tension between crude oil and saline water. The dispersant was mixed with crude prior to its introduction in the capillary tube containing saline water.

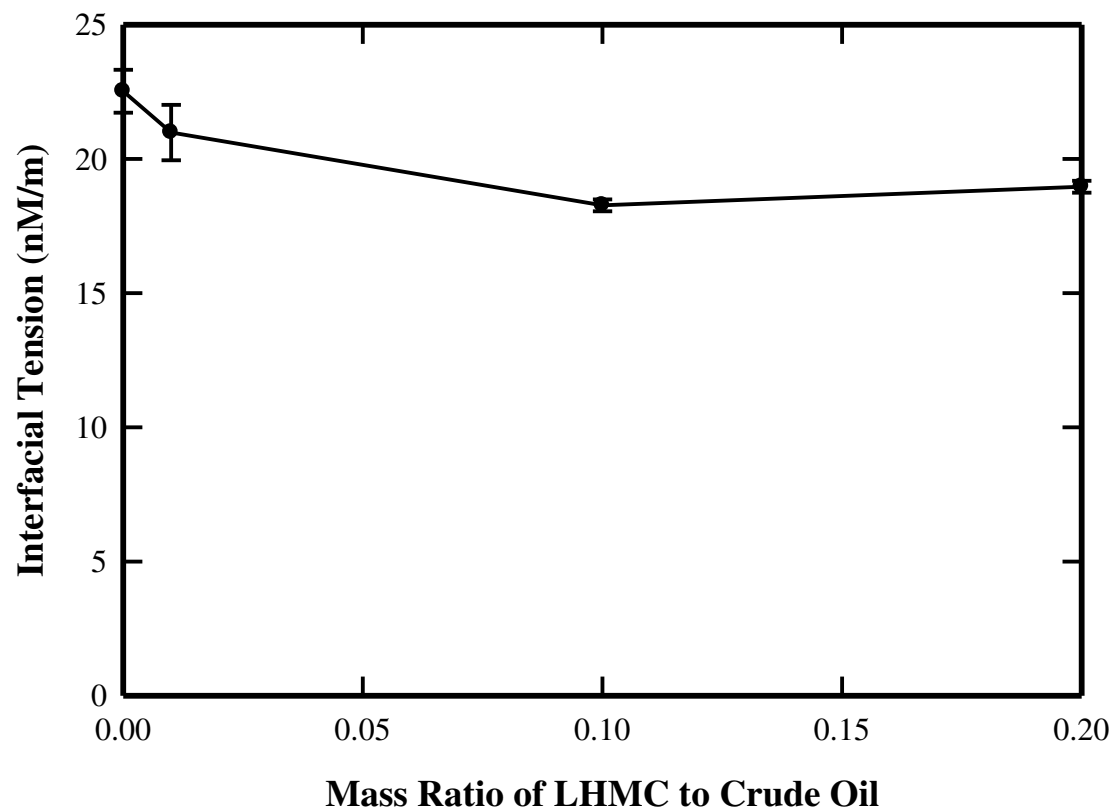


**Figure S-3.** Effect of the amount of LHMC in the absence of dispersant (expressed as the mass ratio of LHMC to crude oil) on the interfacial tension between crude oil and saline water. The pendant drop method was used.

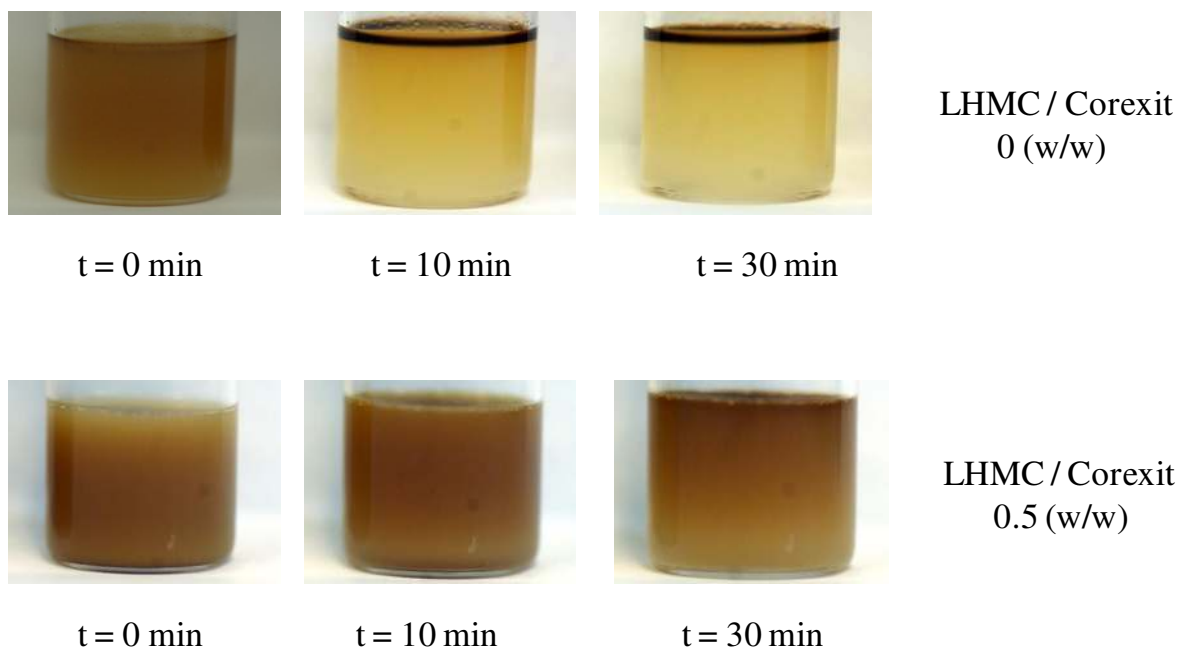


**Figure S-4.** Photographic images showing the increased stability of the crude oil droplets in seawater (pH – 7.9, conductivity – 85 mS/cm) upon the addition of LHM C. The volume ratio of Corexit to crude oil was 0.01. The mass ratio of LHM C to Corexit is 0.5 in the sample shown in the bottom row. Both the samples were stirred together for 30 seconds at 3000 rpm and then left undisturbed on the counter. The vial containing both Corexit and LHM C (bottom row) has more oil dispersed in the aqueous phase after 30 minutes in comparison with the vial containing only Corexit (top row).